A Data Driven Estimate of Glacier Thicknesses Reveals the Influence of Ice Shelves and Other Ocean Interactions

Simon Hans Edasi, Brad Lipovsky

Dept. of Earth & Space Sciences, University of Washington

ABSTRACT. An accurate estimation of glacier volume is essential for effective water resource management and sea-level rise projections, however, traditional methods for assessing glacier thickness are costly and labor-intensive. This study presents a novel approach to estimating glacier thickness utilizing neural networks trained on thickness data from the Glacier Thickness Database (GlaThiDa) and glacier attributes, such as area or slope, from the Randolph Glacier Inventory (RGI). A regression analysis is conducted on a subset of GlaThiDa data, which is then used to infer thicknesses for glaciers in the RGI dataset. Challenges in matching GlaThiDa thickness data to RGI attributes are addressed, employing distance and area thresholds to ensure the matched GlaThiDa thickness is representative of RGI attributes. Furthermore, this study provides a comprehensive comparison with existing global estimates. Notably, this study has lower estimates of volume for shelf and marine-terminating glaciers due to a sparsity of available training data. These findings suggest the neural network effectively models a world without ice shelves and their buttressing effect on ice flow. This departure from previous methods and estimates emphasizes the importance of improved observations of glacier thickness data, particularly in marine environments.

INTRODUCTION

Glacier volume information is crucial for water resource management (Deng and others, 2019; Nolin and others, 2010; Bliss and others, 2014; Frans and others, 2018) and projection of sea level rise (Meier and others, 2007; Zemp and others, 2019). While glacier surface features such as area can be measured remotely, thickness information remains elusive as *in situ* surveys are expensive and labor intensive. Early work by Bahr and others (1997) derived an area-volume scaling relationship which was built upon in subsequent studies, however previous attempts to estimate global glacier volume have been hindered by incomplete datasets (Dyurgerov and others, 2005; Radić and Hock, 2010; Huss and Farinotti, 2012; Grinsted, 2013). While the area-volume scaling relationship derived by Bahr and others (1997) is intended to apply to a population of similar glaciers, these previous studies explore samplings of glaciers such as specific mountain ranges to find new scaling factors for specific ranges of glaciers (Hock and others, 2023).

Two recent studies (Farinotti and others, 2019; Millan and others, 2022) apply different physics-based models on a global scale to estimate a global glacier volume for glaciers contained in the Randolph Glacier Inventory (RGI) (RGI Consortium, 2017) and calibrate their models with data using the Glacier Thickness Database (GlaThiDa) (GlaThiDa Consortium, 2020). This study uses mean scale thicknesses data from GlaThiDa and surface features from RGI to train regression models using shallow neural networks to estimate a mean glacier thickness, and then compares results of these neural networks to recent global estimates by Farinotti and others (2019); Millan and others (2022)

Workflow consists of carrying out a regression analysis on the glaciers contained in the much smaller GlaThiDa data set ($n = 500$) and then using a regression model to infer the thicknesses of the glaciers contained in the much larger RGI data set ($n = 216,501$). Since the GlaThiDa and RGI data sets are not perfectly coincident in time, the datasets are first carefully coregistered. Statistical methods are then described including the use of neural networks from glacier thickness regression and estimation of global glacier volume.

The main result of this study is an estimate of global glacier volume as well as an accounting of glacier volume uncertainty resulting from the statistical model and measured data. This entirely data-driven and physics-free approach to global glacier ice volume achieves statistically similar volume distributions to previous efforts that invoked –to varying degrees– physics-based models (Farinotti and others, 2019; Millan and others, 2022). Adequately complex neural networks can be thought of as universal function approx-

imators (Hornik and others, 1989). In that context, these results suggest that the main limitation of achieving better estimates of glacier thickness is not improvement of models, but rather improving underlying data sets.

BACKGROUND

Efforts to estimate glacier volume go back decades. Early attempts rely on generalized power-law scaling relationships to obtain volume from glacier surface area using 144 glaciers excluding any ice caps and ice sheets (Bahr and others, 1997). Subsequent studies employed these scaling relationships to different datasets with varying results. Dyurgerov and others (2005) monitored the worlds glaciers by estimating mass balance from surface area and included ice caps without referencing any scaling values used. Radić and Hock (2010) upscaled an incomplete glacier inventory using methods from Bahr and Meier (2000) to estimate bias in scaling relationships and establish uncertainty estimations. Grinsted (2013) combined three glacier datasets into a global database and applied area-volume scaling methods. These studies use related techniques, however, they report varied scaling exponents.

Farinotti and others (2019) employs a consensus of five different physics-based models including mass balance, constitutive laws, and flow-line modeling. Millan and others (2022) uses regionally tuned velocity models using high resolution satellite imagery to invert flow velocities for glacier thickness. Farinotti and others (2019); Millan and others (2022) are able to tune their models for estimating ice caps and thus do not exclude them as in previous studies, however, the difference in global volume between the two recent global estimates still arises from a choice to include specific glaciers (Hock and others, 2023).

Data

This project uses mean thickness and mean thickness uncertainty data from GlaThiDa 3.1.0. GlaThiDa contains three separate datasets which describe different scales of measurement. This study uses the "T" dataset which contains mean-scale glacier thicknesses. Glacier features come from the Randolph Glacier Inventory v. 6. No discrimination is made regarding glacier form or termination type for training or estimation.

METHODS

Coregistration

Glacier thickness data from GlaThiDa are combined with surface features from RGI in a process referred to as coregistration. RGI glaciers are matched with GlaThiDa thicknesses using latitude and longitude coordinates contained in both datasets as the only overlapping field between them. These glaciers are matched by finding the minimum distance in RGI to each GlaThiDa Thickness. This process is simple in principle, but some challenges present themselves. First, variable resolution of glacier centroid coordinates in GlaThiDa creates ambiguity in the coregistration process. This location resolution ranges over five orders of magnitude from approximately 1 m to 11 km. As a result of this reduced accuracy multiple GlaThiDa measurements may be associated with a single RGI glacier. In this case, any repeated RGI glaciers are dropped from the final training data. It is also possible for multiple RGI glaciers to be associated with a single GlaThiDa thickness with equal distance between glacier centroids, in which case the GlaThiDa entry is dropped from training. In case multiple RGI glaciers may be associated with a single GlaThiDa glacier, the minimum distance is taken to be a match. In order to reduce uncertainty in these matches with nonzero distance between glacier centroids, the average radius of the glacier, $r = \sqrt{\frac{A^{\mathrm{RGI}}}{\pi}}$, is compared to the minimum distance between glacier centroids, x, to find a relative distance to area ratio $D = \frac{x}{r}$. This distance to area ratio can then be compared to a desirable threshold of uncertainty, T, to exclude erroneous data from training.

The second challenge in dataset coregistration is that the GlaThiDa and RGI data sets are not coincident in time. Significant glacier change may have occurred in the seasons, years, or decades between the GlaThiDa thickness measurement and the RGI data acquisition and labeled thicknesses may be unreliable for a glacier that has changed too much. After matching by centroid location (as described above) a percent difference in size between entries in RGI and GlaThiDa is calculated as,

$$\Delta A_i = \frac{A_i^{\mathrm{RGI}} - A_i^{\mathrm{GlaThiDa}}}{A_i^{\mathrm{GlaThiDa}}}. \quad (1)$$

Throughout this manuscript, the subscript i refers to glaciers in the GlaThiDa catalog. This percent difference represents changes in glacier surface area since thickness surveys were carried out and estimates reliability of the available thickness data. ΔA_i can also be compared to a threshold of uncertainty to dismiss any glaciers that may have unreliable labeled thickness for their measured size.

Four thresholds are tested ($T = 999, 0.25, 0.5, 0.75$) to find the ideal balance between sample size and reliability for training. Estimates made by models trained and validated with data coregistered using each threshold are shown against the survey GlaThiDa thickness in Fig 1. $T = 999$ represents all data regardless of area or location mismatch. This model does not perform well and estimates appear to hover around a mean value. $T = 0.25$ has very poor performance suggesting insufficient data for training. $T = 0.50$ and $T = 0.75$ estimates show improved performance. $T = 0.75$ is selected as the best fit to the data for further analysis.

Neural Networks

A neural network regression model uses interconnected neurons to predict outcomes based on input data. This study uses such models to predict mean glacier thickness from mean scale features available in RGI. Inputs to the model include glacier centroid latitude and longitude, area, slope, elevation, and maximum length. The neural network passes these inputs to interconnected neurons which optimize a regression function to fit mean thickness labels from GlaThiDa to surface features from RGI. It iteratively adjusts the prediction rules to find the best fit, then stops training and saves the optimal model weights as a final model.

With the goal of simplifying parameters of the model, shallow neural networks (SNNs) with two layers of neurons are utilized. The network architecture consists of 6 neurons in the first layer and 2 neurons in the second layer surrounding a 10% dropout normalization layer to help prevent overfitting (Srivastava and others, 2014). Learning rate and validation split are held fixed at 0.01 and 0.2 respectively. Model residuals for the i^{th} GlaThiDa glacier are calculated as,

$$r_i = \hat{h}_i - h_i \tag{2}$$

and fractional residual,

$$R_i = \frac{\hat{h}_i - h_i}{h_i} \tag{3}$$

where h_i is the observed (GlaThiDa-reported) glacier thickness, and $\hat{h}_i$ is the corresponding estimated thickness. Model weights are calculated by minimizing mean absolute error (MAE), $\sum_{i=1}^{N_{\text{GlaThida}}} |r_i| / N_{\text{GlaThida}}$, and mean squared error (MSE) $\sum_{i=1}^{N_{\text{GlaThida}}} r_i^2 / N_{\text{GlaThida}}$, where N_{GlaThida} is the number of glaciers in the GlaThiDa catalog. MAE tells us how the model performs in estimating the average glacier, while MSE is more sensitive to larger errors which allows for discrimination against outliers.

Cross Validation

A requirement for neural networks is division of data into training and testing subsets, which introduces the question of which data to sample for training or testing of the regression model. Results from a single model vary widely depending on which data are sampled to train or validate the model. Rather than optimizing a select set of training and validation data, a single glacier is used to validate a model trained on the remaining coregistered data. Repeating this leave-one-out method for each glacier obtains a distribution of prediction rules, each validated on a unique glacier. The average performance of all models is thus an estimate of a model trained on the full coregistered dataset.

Glacier volume and volume uncertainty calculation

For each of the $N = 216501$ glaciers in the RGI catalog indexed by k, glacier volume is calculated as the product $\hat{V}_k = \hat{H}_k \hat{A}_k$ (no summation on the index k) of the estimated thickness $\hat{H}_k$ and area $\hat{A}_k$. The estimated area $\hat{A}_k$ consists of the RGI-reported area A_k, which is modeled as a normal distribution,

$$\hat{A}_k \sim \mathcal{N}\left[A_k, \text{Var}\left(A_k\right)\right]. \tag{4}$$

Uncertainties due to mapping errors are quantified following the result of Pfeffer and others (2014), who estimated area uncertainty with a simple model of fitting a curve to fractional uncertainties between multiple data sources for RGI. Their approximation yields the relationship

$$\text{Var}\left(A_k\right) \approx c_1 \alpha \left(A_k^{p_1}\right)^2, \tag{5}$$

where A_k is the reported glacier surface area, $\alpha = 0.039$ is the estimated fractional error of a 1 km^2 glacier, $p_1 = 0.70$, and $c_1 = 3$ is a correction factor.

The estimated thickness $\hat{H}_k$ consists of the thickness distribution estimated from the SNN, H_k which is modeled as a normal distribution with mean and variance,

$$\hat{H}_k \sim \mathcal{N}\left[H_k, \text{Var}\left(H_k\right)\right]. \tag{6}$$

The leave one out cross validation of the k^{th} RGI glacier is denoted $\mathcal{H}_{kj}$, indicating that the thickness of RGI glacier k was estimated based on a regression using the entire GlaThiDa database except for glacier j. The expected value of the k^{th} glacier thickness is calculated as,

$$H_k = \frac{1}{N_j} \sum_{j=1}^{N_j} \mathcal{H}_{kj}, \tag{7}$$

where $N_j = 273$ is the number of cross validation iterations.

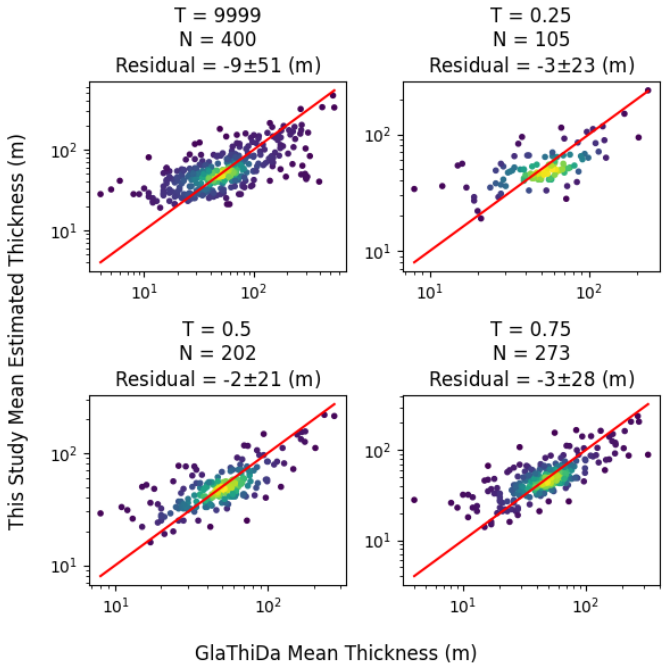

Fig. 1. Testing different coregistration thresholds. GlaThiDa survey thickness compared to this study's estimated thickness on a log scale with a one-to-one fit line shown in red

Thickness uncertainty, $\mathrm{Var}\left(H_k\right)$, is the combination of variances of three sources of uncertainty which are modeled as random variables: reliability of data, $\mathrm{Var}\left(\epsilon_k^{\mathcal{M}}\right)$; uncertainty due to limited thickness data, $\mathrm{Var}\left(\epsilon_k^{\mathcal{H}}\right)$; and model uncertainty, $\mathrm{Var}\left(\epsilon_k^{\mathcal{R}}\right)$.

$$\mathrm{Var}\left(H_k\right) = \mathrm{Var}\left(\epsilon_k^{\mathcal{M}}\right) + \mathrm{Var}\left(\epsilon_k^{\mathcal{H}}\right) + \mathrm{Var}\left(\epsilon_k^{\mathcal{R}}\right). \quad (8)$$

First, reliability of training data is assessed by approximating the measurement uncertainty of data used for training, $\mathrm{Var}\left(\epsilon^{\mathcal{M}}\right)$. This uncertainty is approximated by fitting the mean thickness uncertainty provided in GlaThiDa to the corresponding mean thickness measurement. This model yields the relationship:

$$\sqrt{\mathrm{Var}\left(\epsilon_i^{\mathcal{M}}\right)} \approx c_2 h_i^{p_2}, \quad (9)$$

with constants $c_2 \approx 0.07$ and $p_2 \approx 0.8$. This model is then used to approximate the effect of measurement uncertainty, $\mathrm{Var}\left(\epsilon_k^{\mathcal{M}}\right)$, using H_k as the dependent variable.

Uncertainty due to limited thickness data, $\mathrm{Var}\left(\epsilon_k^{\mathcal{H}}\right)$, is quantified using leave one out cross validation. The variance over the cross validation iterations is given by,

$$\mathrm{Var}\left(\epsilon_k^{\mathcal{H}}\right) \approx \mathrm{Var}_j\left(\mathcal{H}_{kj}\right). \quad (10)$$

Here the notation $\mathrm{Var}(\cdot)$ is used to denote the variance of a random variable and the notation $\mathrm{Var}_j(\cdot)$ to denote the statistical operation of taking the variance of an array of values.

Finally the neural network regression model uncertainty, $\mathrm{Var}\left(\epsilon_k^{\mathcal{R}}\right)$, is approximated by analyzing residuals. A statistical model of residuals is calculated by binning similar thickness estimates h_i into $B < n_i$ bins and for each bin the standard deviation of pooled residuals r_{jB} is calculated as,

$$\sqrt{\mathrm{Var}\left(\epsilon_B^{\mathcal{R}}\right)} \approx \sqrt{\frac{1}{n_B n_j}\sum_{B}^{n_B}\sum_{j}^{n_j}\left(r_{jB} - \bar{r}_B\right)^2}. \quad (11)$$

Due to limited thickness data, some bins must be expanded such that at least 3 glaciers are included to calculate $\mathrm{Var}\left(\epsilon_B^{\mathcal{R}}\right)$. These standard deviations are then fit as a dependent variable to binned thickness measurement h_B in log-log space which yields the relationship,

$$\sqrt{\mathrm{Var}\left(\epsilon_B^{\mathcal{R}}\right)} \approx c_3 h_B^{p_3}, \quad (12)$$

with constants $c_3 = 0.04$ and $p_3 = 0.6$. This statistical model is then used to estimate $\mathrm{Var}\left(\epsilon_k^{\mathcal{R}}\right)$ using H_k as the dependent variable. This approach is similar to the one employed by Farinotti and others (2019) (i.e., their "$1.5\sigma_i/\bar{h}_i$"), with the additional generalization Farinotti and others (2019)

essentially assumed a power law exponent of unity, whereas this study fits this power law exponent from the data. The covariance terms between uncertainties are calculated to be at least two orders of magnitude smaller than the other terms and so they are neglected going forward.

With these distributions in hand, glacier volume variance can be calculated on a glacier-by-glacier basis, for all glaciers in the RGI catalog. For the time being, it is assumed that $\hat{H}_k$ and $\hat{A}_k$ are uncorrelated. In that case, the variance of the k^{th} glacier is calculated as,

$$\begin{aligned}\sigma_k^2 &= \text{Var}(\hat{H}_k \hat{A}_k) \\ &= \text{Var}\left(\hat{H}_k\right)\text{Var}\left(\hat{A}_k\right) + A_k^2\text{Var}\left(\hat{H}_k\right) + H_k^2\text{Var}\left(\hat{A}_k\right)\end{aligned} \tag{13}$$

The sum global volume is considered a random variable with a sampling distribution defined by estimated parameters,

$$\hat{S} \sim \mathcal{N}\left(\sum_k^{N_k}\hat{V}_k, \sum_k^{N_k}\sigma_k^2\right). \tag{14}$$

The sum global volume is approximated as,

$$S \approx \sum_{k=1}^{N_k}\hat{V}_k \pm Z^*_{\alpha/2}\sqrt{\sum_k^{N_k}\sigma_k^2}. \tag{15}$$

RESULTS

The calculation in Equation 15 results in $135.7 \pm 2.4 \times 10^3 \text{km}^3$ of global glacier ice for all glaciers contained in RGI. More than two-thirds of all global ice volume is estimated to be contained in just 377 glaciers, $\approx$ 0.2% of the RGI catalog. Fig 2 compares estimated volumes with Farinotti and others (2019) estimates, and summary statistics are reported for different volumes in Fig 2 representing over or under fitting of previous estimates. Also visible in Fig 2 are a handful of glaciers in Jan Mayen estimated by Farinotti and others (2019) to be on the order of centimeters thick, which is taken to be a model artifact. Table 1 shows a further comparison of estimated volumes by region with Farinotti and others (2019) and Millan and others (2022). Some regions of RGI were combined in Millan and others (2022) and thus are not directly compared.

DISCUSSION

Model Performance

To assess the performance of SNNs, residuals with GlaThiDa are calculated using equations 2 and 3. Estimates are also compared to estimates by Farinotti and others (2019) using their available data. Figure 3 shows residuals of both this study and Farinotti and others (2019). Residuals of both studies show a trend of under-fitting larger thickness and over-fitting smaller thickness. The lowest residuals in both studies are for thicknesses approximately 50 m and residuals are approximately normally distributed with features. The mean residual of this study is -3 ± 28 compared to the mean residual from Farinotti and others (2019) data, 3 ± 33. A t-test of the two distributions of residuals determines they are statistically similar with a p-value of 0.06 with a confidence level of 95%. Fig 3 shows the difference in mean residual comes from the largest thicknesses; this study underestimates these larger thicknesses while Farinotti and others (2019) overestimates these thicknesses to a similar degree.

Thickness and Volume Uncertainty

Uncertainty distributions for glacier thickness and volume are shown in figures 4 and 5. Thickness uncertainty for the smallest estimated thicknesses can vary between 35% to 55%, and percent uncertainty decreases with increasing estimated thickness to roughly 10% for the largest estimated thicknesses. The majority of estimated thicknesses fall between 0.03 and 0.06 km and about 20% to 25% uncertainty. Volume uncertainty increases for the smallest glaciers to a range of 60% to 70% and falls to around 12% to 18% for the largest volumes. Most of the estimated volumes in this study fall between 0.001 to 50 km^3 with uncertainties as high as 50% to as low as 20%. An important distinction between this study and recent global estimates is the accounting of uncertainties. Figure 5 depicts the global sum contributions of propagated uncertainties. 5A shows that cross-validation variance contributes less overall to the global uncertainty than the statistical models used to estimate measurement and model uncertainty. 5B and 5C show the same values scaled by area uncertainty and reported RGI area, respectively. In the calculation for global uncertainty, it is the measurement uncertainty that becomes the most important, followed by uncertainty due to the availability of data as measured by cross-validation. These findings suggest that to improve glacier thickness estimates it is the data that needs to be improved before improving modeling efforts.

Consistency with Previous Estimates

Figure 2 shows a direct comparison with volume estimates from Farinotti and others (2019). The majority of estimated volumes less than 0.1km^3 are higher than Farinotti and others (2019), while volumes greater than 0.1km^3 tend to be lower than Farinotti and others (2019). While these results

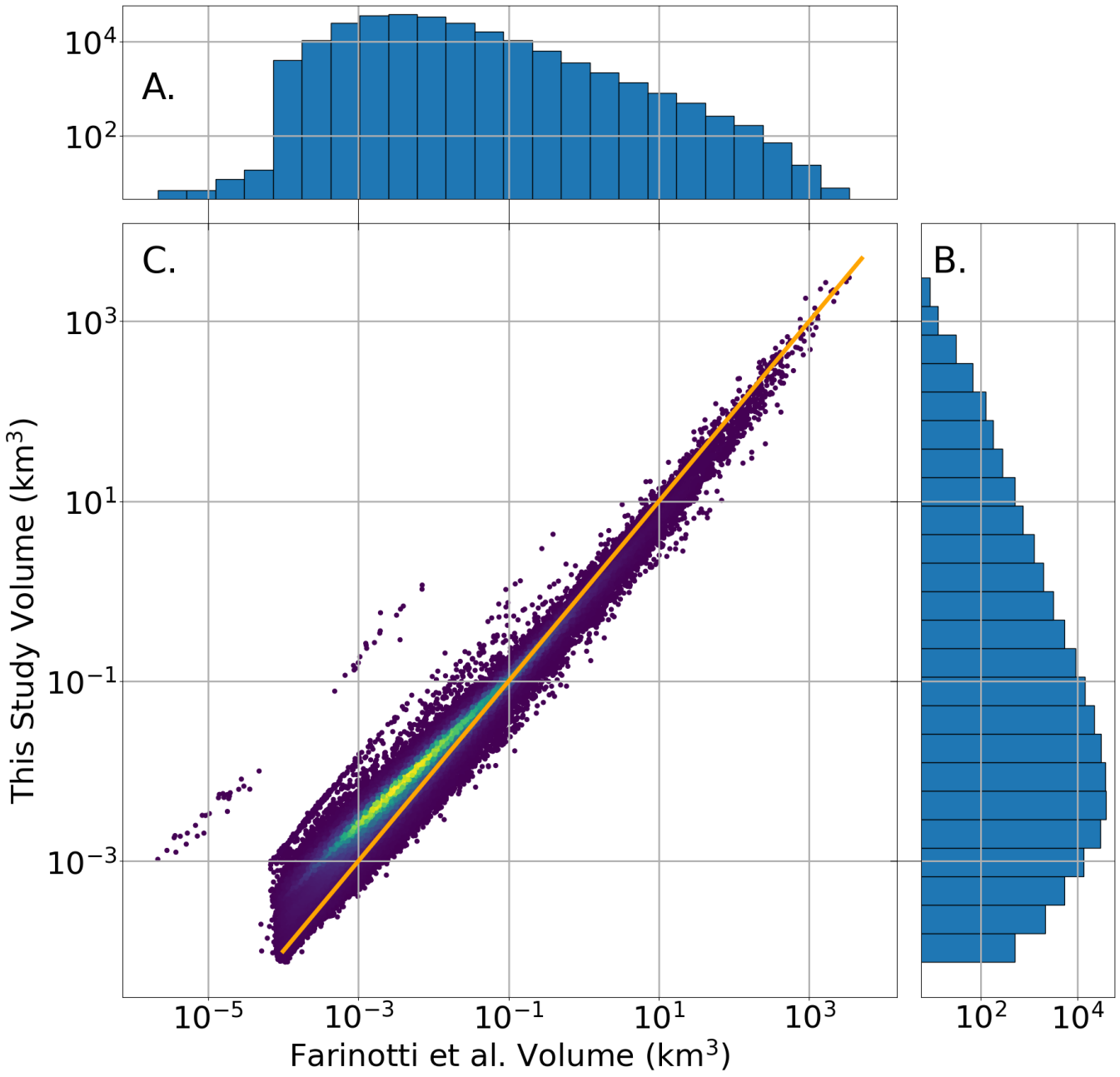

Fig. 2. **A.** Histogram of volumes from Farinotti et al. 2019. **B.**Histogram of volumes from this study. **C.**Direct global comparison between volumes estimated by this study and that of Farinotti et al. 2019 on a log scale with one-to-one perfect fit in orange. Brighter colors represent density of estimates.

Region	Farinotti et al. 2019 (10^3 km^3)	Millan et al. 2022 (10^3 km^3)	This Study (10^3 km^3)
1 Alaska	18.98 +/- 4.92	* +/- *	19.91 +/- 1.65
2 Western Canada and US	1.06 +/- 0.27	* +/- *	0.83 +/- 0.06
3 North Canadian Arctic	28.33 +/- 7.35	25.4 +/- 7.2	21.6 +/- 1.32
4 South Canadian Arctic	8.61 +/- 2.23	7.0 +/- 2.1	5.3 +/- 0.5
5 Greenland Periphery	15.69 +/- 4.07	11.8 +/- 3.7	25.21 +/- 3.0
6 Iceland	3.77 +/- 0.98	3.7 +/- 0.9	2.38 +/- 0.38
7 Svalbard and Jan Mayen	7.47 +/- 1.94	7.0 +/- 2.3	5.49 +/- 0.37
8 Scandinavia	0.3 +/- 0.08	0.29 +/- 0.1	0.18 +/- 0.01
9 Russian Arctic	14.64 +/- 3.8	15.5 +/- 3.9	7.88 +/- 0.5
10 North Asia	0.14 +/- 0.04	0.09 +/- 0.05	0.16 +/- 0.01
11 Central Europe	0.13 +/- 0.03	0.12 +/- 0.05	0.1 +/- 0.01
12 Caucus and Middle East	0.06 +/- 0.02	0.06 +/- 0.03	0.06 +/- 0.005
13 Central Asia	3.27 +/- 0.85	* +/- *	3.34 +/- 0.15
14 South West Asia	2.87 +/- 0.74	* +/- *	3.18 +/- 0.3
15 South East Asia	0.88 +/- 0.23	* +/- *	0.91 +/- 0.03
16 Low Latitudes	0.1 +/- 0.03	0.07 +/- 0.04	0.06 +/- 0.003
17 Southern Andes	5.34 +/- 1.39	5.9 +/- 1.6	4.42 +/- 0.4
18 New Zealand	0.07 +/- 0.02	0.07 +/- 0.03	0.09 +/- 0.01
19 Antarctic and Subantarctic	46.47 +/- 12.06	35.1 +/- 9.1	34.55 +/- 3.11

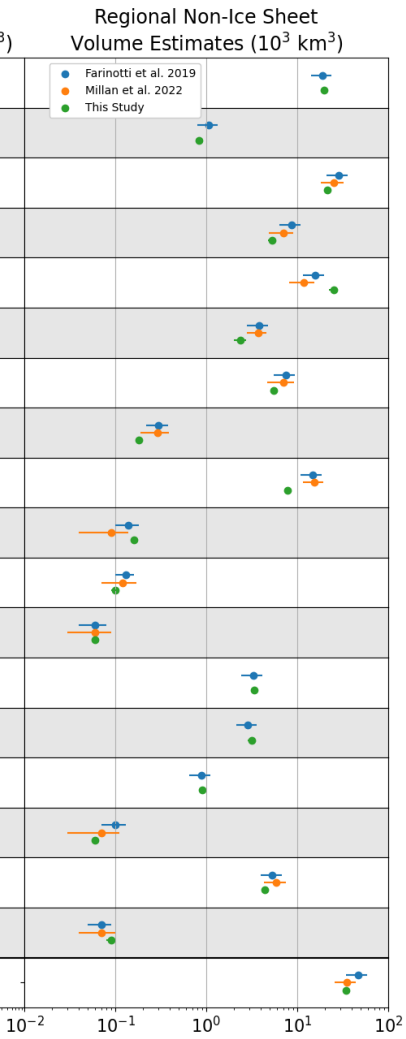

Table 1. Table of RGI regional volume comparisons between Farinotti and others (2019), Millan and others (2022), and this study. Millan and others (2022) combined Alaska and Western Canada (RGI 1, 2 respectively) into a single region, as well as high-mountain Asia (RGI regions 13,14,15) into a single region making it not possible to compare these regions.

Table 2. Glacier volumes 1×10^{-5} to 1×10^{4} km^3. These glacier volume estimates sum to 135.7×10^{3} km^3 and the entirety of glaciers contained in RGI. Volume difference and percent volume difference represent the difference between this study's estimate and Farinotti and others (2019).

	Area (km^2)	Thickness Estimate (m)	Volume Difference (km^3)	Percent Volume Difference
mean	3.446	40	−0.2	25.6
median	0.252	38	0.0	34.1
STD	51.081	18	5.9	38.7
min	0.010	7	−661.6	−750.0
max	7537.579	893	1019.5	100.0
count	216 501	216 501	216 501	216 501

Table 3. Glacier volumes 1×10^{-5} to 1×10^{-1} km^3. These glacier volume estimates sum to 2.9×10^{3} km^3 and represent 88.4% of glacier population and 2.1% of global volume. Glaciers of this volume tend to have higher estimated volume than Farinotti and others (2019). Volume difference and percent volume difference represent the difference between this study's estimate and Farinotti and others (2019).

	Area (km^2)	Thickness Estimate (m)	Volume Difference (km^3)	Percent Volume Difference
mean	0.390	36	0.0	32.5
median	0.201	36	0.0	38.5
STD	0.470	11	0.0	32.1
min	0.010	7	−0.6	−750.0
max	8.399	138	0.1	100.0
count	191 362	191 362	191 362	191 362

Table 4. Glacier volumes 1×10^{-1} to 50 km^3. These glacier volume estimates sum to 35.4×10^{3} km^3 and represent 11.4% of glacier population and 26.1% of global volume. Glaciers of this volume tend to have lower estimated volume than Farinotti and others (2019). Volume difference and percent volume difference represent the difference between this study's estimate and Farinotti and others (2019).

	Area (km^2)	Thickness Estimate (m)	Volume Difference (km^3)	Percent Volume Difference
mean	14.552	63	−0.8	−27.6
median	5.008	57	0.0	−19.7
STD	31.298	23	4.0	43.1
min	0.833	15	−225.4	−688.2
max	774.565	311	13.8	100.0
count	24 761	24 761	24 761	24 761

Table 5. Glacier volumes 50 to 1 $\times$ 10^3 km^3. These glacier volume estimates sum to 61.8 $\times$ 10^3 km^3 and represent 0.2% of glacier population and 45.6% of global volume. Glaciers of this volume tend to have lower estimated volume than Farinotti and others (2019). Volume difference and percent volume difference represent the difference between this study's estimate and Farinotti and others (2019).

	Area (km^2)	Thickness Estimate (m)	Volume Difference (km^3)	Percent Volume Difference
mean	672.042	238	−54.8	−41.1
median	496.930	225	−39.7	−36.1
STD	474.811	63	88.5	48.7
min	218.943	81	−661.6	−350.6
max	3266.694	436	156.1	52.1
count	358	358	358	358

Table 6. Glacier volumes 1 $\times$ 10^3 to 1 $\times$ 10^4 km^3. These glacier volume estimates sum to 35.5 $\times$ 10^3 km^3 and represent 0.009% of glacier population and 26.2% of global volume. Glaciers of this volume tend to have similar estimated volume with Farinotti and others (2019). Volume difference and percent volume difference represent the difference between this study's estimate and Farinotti and others (2019).

	Area (km^2)	Thickness Estimate (m)	Volume Difference (km^3)	Percent Volume Difference
mean	3713.457	517	53.1	1.5
median	3362.656	468	−0.1	−1.1
STD	1328.140	133	484.0	24.0
min	2219.510	306	−624.9	−37.6
max	7537.579	893	1019.5	46.0
count	19	19	19	19

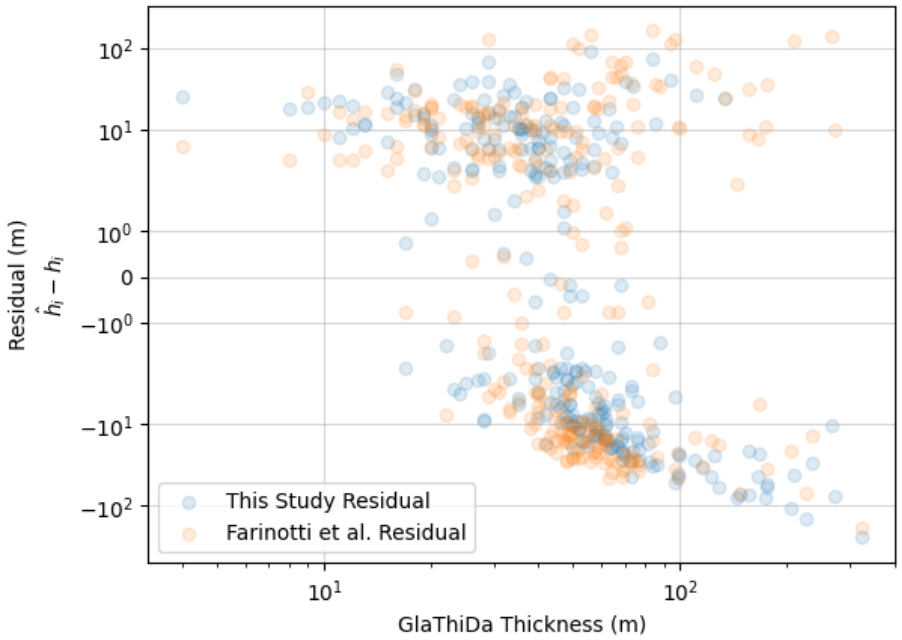

Fig. 3. Plot of residuals of both this study (blue) and Farinotti et al. 2019 (orange) against corresponding survey thickness found in GlaThiDa on a log-log scale. Residuals are calculated as estimated thickness minus thickness measurement found in GlaThiDa.

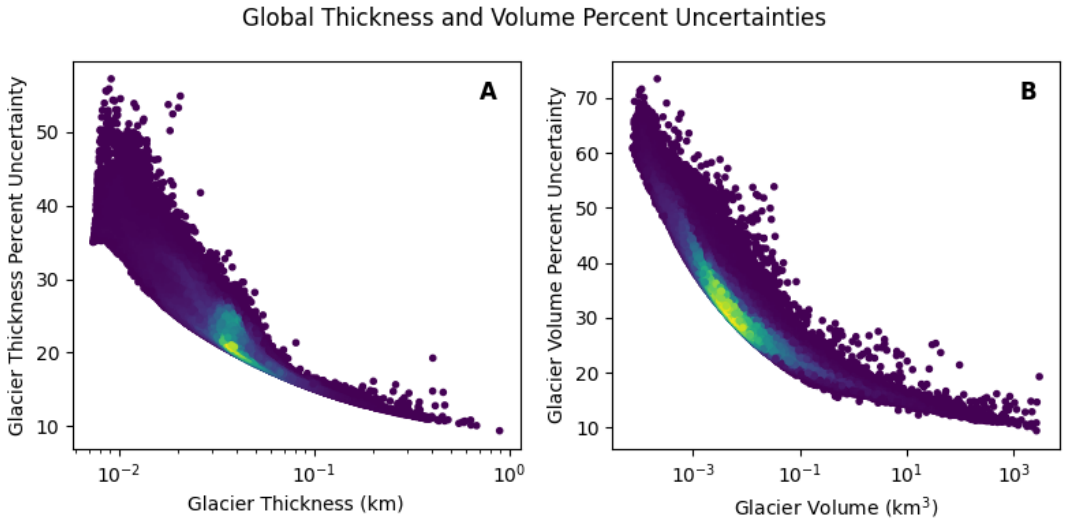

Fig. 4. **A.** Percent uncertainty for each mean glacier thickness estimate. Brighter colors represent density of estimates. **B.** Percent uncertainty for each estimated glacier volume. Color scheme is same as **A.**

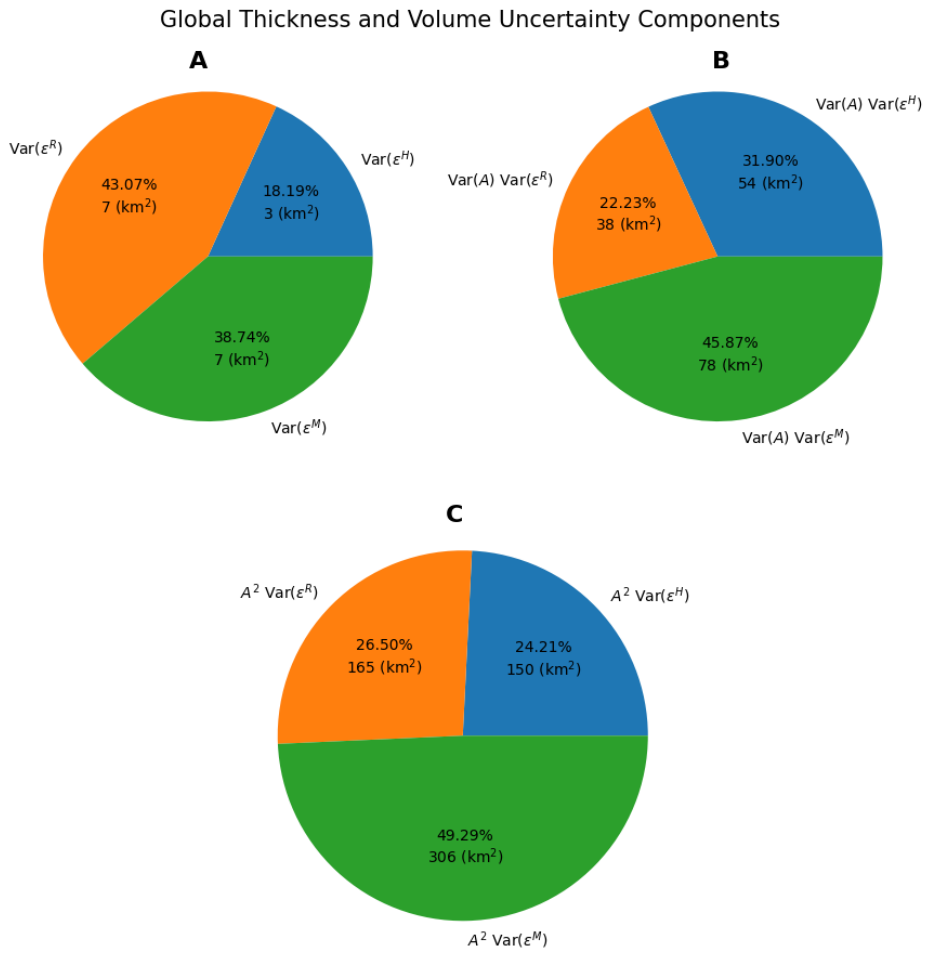

Fig. 5. Pie charts depicting uncertainty components. **A.** Components of global thickness uncertainty, each one the variance of a source of uncertainty modeled as a random variable. Var $\left(\epsilon^{\mathcal{M}}\right)$ represents uncertainty concerning the reliability of training data. Var $\left(\epsilon^{\mathcal{H}}\right)$ measures the variance of the leave one out cross validation method and approximates uncertainty due to limited training data. Var $\left(\epsilon^{\mathcal{R}}\right)$ is an approximation of model uncertainty and is calculated using binned residuals. **B.** Components of Var (A) Var (H) term of global volume uncertainty. **C.** Components of A^2Var (H) term of global volume uncertainty.

show that both this study and Farinotti and others (2019) achieve similar results when compared to GlaThiDa measurements, examination of residudals show that Farinotti and others (2019) overestimates larger glacier thicknesses to a similar degree that this study underestimates them. The estimate of this study for the global sum of glacier volume is within the global uncertainty bounds of Farinotti and others (2019); Millan and others (2022), though regional estimates vary widely (Figure 1). Specifically, estimates from this study fall below the uncertainty bounds for Farinotti and others (2019); Millan and others (2022) for RGI regions 6 (Iceland), 8 (Scandinavia), 9 (Russian Arctic), and 19 (Antarctic and Subantarctic). This study estimates higher volumes than Farinotti and others (2019); Millan and others (2022) for RGI region 5 (Greenland Periphery). Regions 9 and 19 have the highest sum and mean glaciated area, and they are the regions with the highest discrepancy. Greenland on the other hand, has about 10% of the mean glaciated area and similar sum glaciated area to 9 and 19. Further, the mean disagreement within the Greenland Periphery is near 0 while the sum discrepancy is actually one of the most negative. This suggests the SNNs are estimating very high volumes for a few glaciers in the Greenland Periphery. Meanwhile, regions 9 and 19 contain several glaciers that are shelf-terminating according to RGI. This shelf-termination can buttress the glacier flow and allow thickness distributions to be thicker than a standard alpine glacier that is allowed to flow freely. While this buttressing effect is often studied in the context of ice sheets (Dupont and Alley, 2005; Sun and others, 2020; Pegler, 2018; Pritchard and others, 2012), the results from the SNNs suggest similar effects on non-ice-sheet glaciers.

This study estimates a mean thickness for each glacier contained in RGI, however, previous studies exclude particular glaciers for various reasons (Hock and others, 2023). Comparing glacier volumes estimated by this study to those from Farinotti and others (2019) reduces the global volume estimate to $121.85 \times 10^3 \text{km}^3$, approximately $28 \times 10^3 \text{km}^3$ less than Farinotti and others (2019). Additionally, Millan and others (2022) excludes Antarctic glaciers supported by the ice shelf. By excluding these glaciers from RGI, the sum volume estimate becomes $111.399 \times 10^3 \text{km}^3$, approximately $29 \times 10^3 \text{km}^3$ less than Millan and others (2022). Estimated glacier thicknesses are comparable to the mean of the estimates provided by Farinotti and others (2019), and find that nearly 70% of the difference between the two studies can be accounted for by 1000 of the 215519 glaciers available from Farinotti and others (2019). Of the 100 most negative volume differences, 42 are ice caps in various regions and 40 are coded in RGI as shelf supported glaciers in Antarctica.

One further discrepancy between this global estimate and the previous estimates of Farinotti and others (2019) and Millan and others (2022) is the size of confidence intervals for the sum volume. Farinotti and others (2019) describe a method of weighting five glacier thickness models based on deviations from calibration data, resulting in an uncertainty that reflects disagreement between consensus models. Millan and others (2022) produce maps of distributed thickness and thickness uncertainty while citing an average uncertainty across regions, which represents perturbations to a single model. These sources of variability are considerably different from what has been quantified in this study, and lack of discussion of previous uncertainty estimates makes a direct comparison extremely difficult.

Marine-Terminating Glaciers and Shelf-Supported Ice Caps

Considerable interest surrounds the stability of marine ice sheets (Bassis and others, 2024) due to the possibility of rapid sea level rise associated with the marine ice sheet instability (Schoof, 2007; Katz and Worster, 2010; Pegler, 2018). The recent Antarctic BUttressing Model Intercomparison Project (ABUMIP) has specifically sought to describe the response of the Antarctic Ice Sheet to the removal of the supporting ice shelves (Sun and others, 2020) following ice shelf collapse (Scambos and others, 2004; Rignot and others, 2004; Banwell and others, 2013). Here, we find a negative glacier volume bias for marine icecaps and glaciers that feed into floating ice shelves. This bias occurs because the coregistered training dataset (GlaThiDa glacier-level "T" data) is non-representative; it does not contain any ice shelf-supported glaciers. For this reason, we interpret the SNNs as having been trained to represent glacier thickness without ice shelves. We therefore offer the novel interpretation that these glacier thickness estimates reflect an estimate for the thickness as if ice shelves have been removed. In this way, this statistical approach is essentially a data-driven analogy to the ABUMIP project.

Although the demise of ice shelves has been studied widely in the context of the Antarctic Ice Sheet, this process has been less well quantified in the context of non-ice sheet glaciers and smaller marine icecaps. The discrepancy between our ice volume estimate and that of Farinotti and others (2019) is $\sim 29 \times 10^3$ km^3, equivalent to about 7.1 cm of sea level rise (SLR). The assessed contribution from non-ice sheet glaciers to sea level rise ranges from 12 to 29 cm (low warming scenario) to 32 cm in a high warming scenario (Table 9.11, Fox-Kemper, 2021). The estimated 7.1 cm SLR contribution from the loss of ice shelf buttressing and other ocean interactions to non-ice sheet glaciers therefore constitutes between 22% and 59% of the glacier contribution to SLR.

CONCLUSIONS

This study estimates a global ice volume using a purely data-driven approach eschewing all physics. The resulting global ice volume estimate is lower than previously published studies. The cause of the discrepancy stems from a lack of available and reliable training data; few marine-influenced icecaps and no glaciers with ice shelves are in the coregistered dataset. One conclusion to be drawn from this result is that a more representative dataset including such glaciers would benefit future estimate of global ice volume. These results also suggest the novel interpretation that these lower estimate of ice volume gives insights into a possible future where marine icecaps and glaciers supported by ice shelves have experienced ice shelf collapse and attained a new study state with lower total grounded ice volume.

REFERENCES

Bahr DB and Meier MF (2000) Snow patch and glacier size distributions. *Water Resources Research*, **36**(2), 495–501

Bahr DB, Meier MF and Peckham SD (1997) The physical basis of glacier volume-area scaling. *Journal of Geophysical Research: Solid Earth*, **102**(B9), 20355–20362

Banwell AF, MacAyeal DR and Sergienko OV (2013) Breakup of the larsen b ice shelf triggered by chain reaction drainage of supraglacial lakes. *Geophysical Research Letters*, **40**(22), 5872–5876

Bassis JN, Crawford A, Kachuck SB, Benn DI, Walker C, Millstein J, Duddu R, Åström J, Fricker H and Luckman A (2024) Stability of ice shelves and ice cliffs in a changing climate. *Annual Review of Earth and Planetary Sciences*, **52**

Bliss A, Hock R and Radić V (2014) Global response of glacier runoff to twenty-first century climate change. *Journal of Geophysical Research: Earth Surface*, **119**(4), 717–730

Deng H, Chen Y and Li Y (2019) Glacier and snow variations and their impacts on regional water resources in mountains. *Journal of Geographical Sciences*, **29**, 84–100

Dupont T and Alley R (2005) Assessment of the importance of ice-shelf buttressing to ice-sheet flow. *Geophysical Research Letters*, **32**(4)

Dyurgerov MB, Meier MF and others (2005) *Glaciers and the changing Earth system: a 2004 snapshot*, volume 58. Institute of Arctic and Alpine Research, University of Colorado Boulder

Farinotti D, Huss M, Fürst JJ, Landmann J, Machguth H, Maussion F and Pandit A (2019) A consensus estimate for the ice thickness distribution of all glaciers on earth. *Nature Geoscience*, **12**(3), 168–173

Fox-Kemper B (2021) Ocean, cryosphere and sea level change. In *AGU fall meeting abstracts*, volume 2021, U13B–09

Frans C, Istanbulluoglu E, Lettenmaier DP, Fountain AG and Riedel J (2018) Glacier recession and the response of summer streamflow in the pacific northwest united states, 1960–2099. *Water Resources Research*, **54**(9), 6202–6225

GlaThiDa Consortium (2020) Glacier thickness database (glathida) 3.1.0 (doi: 10.5904/wgms-glathida-2020-10)

Grinsted A (2013) An estimate of global glacier volume. *The Cryosphere*, **7**(1), 141–151

Hock R, Maussion F, Marzeion B and Nowicki S (2023) What is the global glacier ice volume outside the ice sheets? *Journal of Glaciology*, **69**(273), 204–210

Hornik K, Stinchcombe M and White H (1989) Multilayer feedforward networks are universal approximators. *Neural networks*, **2**(5), 359–366

Huss M and Farinotti D (2012) Distributed ice thickness and volume of all glaciers around the globe. *Journal of Geophysical Research: Earth Surface*, **117**(F4)

Katz RF and Worster MG (2010) Stability of ice-sheet grounding lines. *Proceedings of the Royal Society A: Mathematical, Physical and Engineering Sciences*, **466**(2118), 1597–1620

Meier MF, Dyurgerov MB, Rick UK, O'neel S, Pfeffer WT, Anderson RS, Anderson SP and Glazovsky AF (2007) Glaciers dominate eustatic sea-level rise in the 21st century. *Science*, **317**(5841), 1064–1067

Millan R, Mouginot J, Rabatel A and Morlighem M (2022) Ice velocity and thickness of the world's glaciers. *Nature Geoscience*, **15**(2), 124–129

Nolin AW, Phillippe J, Jefferson A and Lewis SL (2010) Present-day and future contributions of glacier runoff to summertime flows in a pacific northwest watershed: Implications for water resources. *Water Resources Research*, **46**(12)

Pegler SS (2018) Suppression of marine ice sheet instability. *Journal of Fluid Mechanics*, **857**, 648–680

Pfeffer WT, Arendt AA, Bliss A, Bolch T, Cogley JG, Gardner AS, Hagen JO, Hock R, Kaser G, Kienholz C and others (2014) The randolph glacier inventory: a globally complete inventory of glaciers. *Journal of glaciology*, **60**(221), 537–552

Pritchard H, Ligtenberg SR, Fricker HA, Vaughan DG, van den Broeke MR and Padman L (2012) Antarctic ice-sheet loss driven by basal melting of ice shelves. *Nature*, **484**(7395), 502–505

Radić V and Hock R (2010) Regional and global volumes of glaciers derived from statistical upscaling of glacier inventory data. *Journal of Geophysical Research: Earth Surface*, **115**(F1)

RGI Consortium (2017) Randolph glacier inventory - a dataset of global glacier outlines, version 6 (doi: 10.7265/4m1f-gd79)

Rignot E, Casassa G, Gogineni P, Krabill W, Rivera A and Thomas R (2004) Accelerated ice discharge from the antarctic peninsula following the collapse of larsen b ice shelf. *Geophysical research letters*, **31**(18)

Scambos TA, Bohlander J, Shuman CA and Skvarca P (2004) Glacier acceleration and thinning after ice shelf collapse in the larsen b embayment, antarctica. *Geophysical Research Letters*, **31**(18)

Schoof C (2007) Ice sheet grounding line dynamics: Steady states, stability, and hysteresis. *Journal of Geophysical Research: Earth Surface*, **112**(F3)

Srivastava N, Hinton G, Krizhevsky A, Sutskever I and Salakhutdinov R (2014) Dropout: a simple way to prevent neural networks from overfitting. *The journal of machine learning research*, **15**(1), 1929–1958

Sun S, Pattyn F, Simon EG, Albrecht T, Cornford S, Calov R, Dumas C, Gillet-Chaulet F, Goelzer H, Golledge NR and others (2020) Antarctic ice sheet response to sudden and sustained ice-shelf collapse (abumip). *Journal of Glaciology*, **66**(260), 891–904

Zemp M, Huss M, Thibert E, Eckert N, McNabb R, Huber J, Barandun M, Machguth H, Nussbaumer SU, Gärtner-Roer I and others (2019) Global glacier mass changes and their contributions to sea-level rise from 1961 to 2016. *Nature*, **568**(7752), 382–386